

Avalanche-mediated transport in a rotated granular mixture

Vidar Frette and Joel Stavans

Department of Physics of Complex Systems, The Weizmann Institute of Science, Rehovot 76 100, Israel

(Received 12 February 1997; revised manuscript received 5 May 1997)

A binary mixture of granular materials in a horizontal, rotating tube segregates under certain circumstances into an alternating pattern of bands of two types along the tube axis, each type being rich in one of the components. The pattern coarsens with time through band shrinking and merging, until a steady state characterized by some average bandwidth is reached. We have studied experimentally the long-term evolution of segregation patterns in sand-glass bead mixtures. We observe that during coarsening, the two types of band evolve differently, indicating that another transport mechanism is at work besides diffusion. We propose that glass beads are transported axially due to ‘‘avalanche waves,’’ a hallmark of the discontinuous flow characterizing sand-rich bands. [S1063-651X(97)01612-7]

PACS number(s): 82.70.-y, 46.10.+z, 64.60.Ht, 02.50.Ey

I. INTRODUCTION

Powders with grains that vary in size, density, or surface properties will often segregate into regions rich in some of the components while flowing or being vibrated. Landslides and conveyors are examples of natural and practical situations where segregation occurs. In many applications, such as in the manufacturing of pharmaceuticals or cement, one needs to keep a granular mixture homogeneous, but segregation is often hard to avoid. Despite its importance in these and other applications and the considerable amount of research that has been carried out, segregation processes are still poorly understood. Several microscopic (grain-level) mechanisms have been proposed to explain segregation. One example is the ‘‘random fluctuation sieve’’ [1], in which each layer in a gravity-driven surface flow is seen as a rapidly varying sieve, through which particles of smaller sizes may fall. This leads to an accumulation of large particles at the top. Another example is the model for quasistatic situations such as the filling of a silo or the building up of a pile in Ref. [2]. Here grains are added one by one and allowed to roll along the granular packing until a stable site is reached. Since smaller grains come to rest more easily, more large grains reach the vicinity of the silo walls and therefore their concentration there increases. Other approaches to surface segregation include the use of cellular automata [3] and variational formulations of bulk mechanics [4].

We have studied segregation of granular media in a half-filled, horizontal, rotating tube, in which binary mixtures of powders form alternating bands of different composition along the drum’s axis, as shown in Fig. 1. Under rotation the

material forms a slope characterized by a composition-dependent average angle to the horizontal. This so-called dynamical angle of repose differs from the static angle of repose in a pile in that it also depends on rotation frequency. Grains at the top of the slope flow downward under the influence of gravity. This flow takes place within a thin surface layer, while the rest of the material rotates like a solid.

One advantage of this system over other granular flows that display segregation is that the rotation can be applied uniformly over very long time periods, as opposed to the highly inhomogeneous convection currents in vibrated layers. Moreover, quasi-one-dimensional patterns are generated in this system and the evolution of the process can therefore be mapped in detail.

Evidence for axial segregation in horizontal rotating tubes was reported by Oyama [5]. Donald and Roseman studied segregation in small-aspect-ratio (length-to-diameter) tubes using 30 different binary mixtures of sand, salt, and glass beads. They concluded that banding results when the static angles of repose of the small (large) particles θ_s (θ_l) obey the inequality $\theta_s > \theta_l$. They also claimed that the segregation starts near the tube boundaries [6]. This claim formed the basis of a model by Bridgewater, Sharpe, and Stocker, who predicted that the higher friction at the boundaries leads to a steeper slope in their vicinity and consequently to a depletion of the more mobile large particles near the boundaries [7]. Das Gupta and co-workers investigated the effects of varying the rotation frequency in small-aspect-ratio tubes when using mixtures of sand of two different particle sizes. They concluded that the aforementioned inequality between the static angles of repose of small and large grains should be replaced



FIG. 1. Horizontal tube ($L = 16.2$ cm) half filled with a granular mixture. Under rotation the mixture segregates into bands rich in each component. Note the difference in angle of repose between the two types of bands. White bands are wider at the top and bottom as compared to the middle. The arrow indicates the front of an ‘‘avalanche wave’’ (see the text) propagating to the right. The experiment used a 50-50 mixture of 0.29-mm (white) glass beads and (black) sand. This pattern of glass-rich white bands and sand-rich black bands appeared after 3930 revolutions at 13.1 rpm.

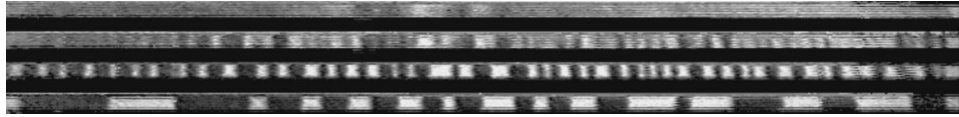


FIG. 2. Four stages in the evolution of an experiment with system size $L = 46.2$ cm started from a homogeneous mixture of black material and 0.44-mm spheres. The angular velocity was 15.5 rpm. The tube is shown (a) initially and after (b) 15, (c) 80, and (d) 49 600 revolutions, respectively.

by a condition on the frequency-dependent dynamic angles of repose as a criterion for the occurrence of the banding instability. Since these vary differently with frequency for different grains sizes or types, a mixture showed the banding instability only in certain frequency ranges and not in others. After the formation of small bands, the latter coarsened until an average bandwidth was reached. They observed a monotonic increase of this quantity with increasing rotation frequency [8]. Hill and Kakalios reported experiments in which the difference between the dynamic angles of repose of the mixed state and the more mobile grains approached zero as the rotation rate was reduced. For their system (glass beads of different sizes) they were able to restore the homogeneously mixed state after segregation had occurred by lowering the angular velocity [9]. More recently, Hill, Caprihan, and Kakalios used magnetic resonance imaging to monitor the interior of the granular material and found that surface observations do not always reflect fully the extent of segregation in the bulk [10]. Zik *et al.* performed experiments with mixtures of sand and glass beads, for which the difference in angle of repose is considerably more marked than in mixtures of sand particles. Using large-aspect-ratio (length-to-diameter) tubes, they observed nucleation of bands to appear roughly at the same time all along the tube, in contrast to previous claims [6]. Experiments with mixtures of monodisperse glass beads of different size ratios were also performed in order to isolate the effect of size on the segregation process. In contrast to the results reported in Ref. [9], no segregation into bands was observed [11]. Interestingly, Nakagawa has reported axial segregation in experiments using sand grains with a continuous size distribution. However, the initial band patterns were much less reproducible. Furthermore, he observed a size distribution in the axial direction for each band [12]. All these studies have been concerned mainly with the early stages of band formation.

Existing theoretical studies have accounted for axial segregation in terms of a diffusion process [8,9,11,13]. In this picture band formation is a result of an effective negative diffusion coefficient arising from differences in angles of repose. Other models have dealt with the simpler geometries, e.g., a rotated two-dimensional drum [14] or the filling of a two-dimensional silo [15], in order to understand radial segregation, a precursor of axial segregation.

In contrast to previous experimental work, we focus in

this paper on the characterization of the long-term evolution of the band pattern in large-aspect-ratio tubes. We have used powders that exhibit continuous (glass beads) versus punctuated avalanche flow (sand grains). This has enabled us to identify a transport mechanism involving “avalanche waves” that mediates the exchange of material between glass bands through wide sand-rich bands. This mechanism is markedly different from the diffusion picture on which previous investigations were based. In spite of the noisy behavior of the avalanches, this transport mechanism is surprisingly persistent and can have a strong influence on the coarsening process of the band pattern.

The experimental setup is described in Sec. II and the experiments that have been carried out are described in Sec. III. The discussion in Sec. IV focuses on the avalanche waves, but we also mention other dynamical phenomena that have been observed in this system. A summary is given in Sec. V.

II. EXPERIMENTAL SETUP

Our experiments were performed in horizontal rotating glass tubes with an inner diameter $D = 1.1$ cm and a length L of either 46 cm or 16 cm, corresponding to $L/D = 42$ and 15, respectively. The granular mixture consisted of black sand and white glass beads. The grains of sand had irregular shape and were sieved to select a fraction with size between 0.147 mm and 0.208 mm. The nearly spherical glass beads had diameters of 0.29 ± 0.03 mm or 0.44 ± 0.03 mm. In terms of the average sand grain size $d = 0.178$ mm the tube diameter was $D/d = 62$. All experiments were carried out with the tube half filled with granular material, precluding any core of material that never reaches the surface [16]. The dynamical angle of repose in glass-rich bands is lower than in sand-rich band. The bands rich in glass run smoothly, while the bands rich in sand flow discontinuously in the form of avalanches.

In the experiments to be described below, the rotation frequency was 13–15 rpm. A series of experiments performed over a range in frequency indicated that this parameter does not have a strong influence on the band evolution and that the number of revolutions is the relevant parameter. At 14 rpm, the nondimensional ratio $(D/\tau^2)/g \sim 2 \times 10^{-4}$ (here τ is the time it takes for a grain to complete one



FIG. 3. Four stages in the evolution of an experiment with system size $L = 45.7$ cm. Initially, the left (right) part of the tube was filled with pure white (black) material (0.29-mm white glass spheres were used). The angular velocity was 14.3 rpm. The tube is shown (a) at the start of the experiment and after (b) 48 700, (c) 111 000, and (d) 255 000 revolutions, respectively.

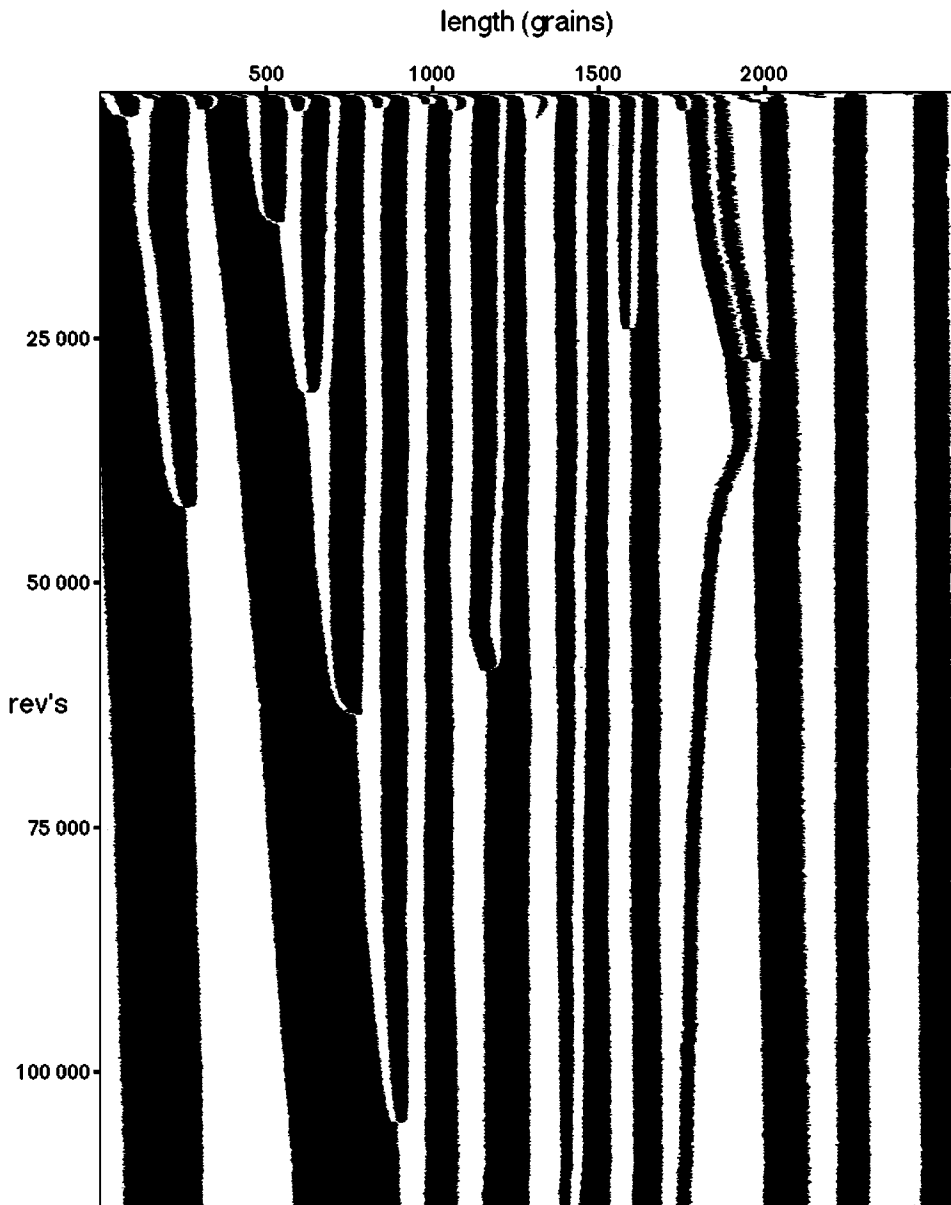


FIG. 4. Space-time diagram for the experiment in Fig. 2 showing coarsening of the band pattern. The distance along the tube is given in terms of the average sand grain diameter. The diagram covers 123 h (114 000 revolutions). The fluxes of white material through the leftmost two (drifting) black bands (referring to the end of the experiment) were 0.10 sphere/rev and 0.23 sphere/rev, respectively (these estimates were obtained between revolutions 66 000 and 90 000).

“round” in the tube and g is the acceleration of gravity). Therefore, centrifugal and Coriolis forces were negligible in our experiments. The granular flow was recorded using a charge coupled device camera and a video recorder in either real-time or time-lapse mode.

We use space-time diagrams to give a succinct description of the long-term evolution of the band patterns. These diagrams were generated by reading out horizontal lines (one pixel wide) running along the axis of the tube at fixed time intervals and stacking them vertically. The downward direction in the diagrams corresponds to increasing time. In some of the runs, views from a tilted mirror beneath the tube were recorded throughout the experiment in order to follow in detail the wave motion at the lower edge in the sand bands. Image processing was carried out using National-Institute-of-Health Image (public domain).

III. EXPERIMENTS

Figure 2 shows a sequence of snapshots of the tube starting from a nearly homogeneous mixture [Fig. 2(a)]. After a few rotations, inhomogeneities appear in the mixture [Fig. 2(b)], which develop into bands containing predominantly glass or sand [Fig. 2(c)]. These bands appear to be homogeneous in the axial as well as azimuthal direction. Note the rather uniform spacing of these bands. In the ensuing coarsening process, some bands shrink and finally disappear, while others grow at their expense, and a more irregular pattern of bands arises [Fig. 2(d)].

This coarsening process does not lead to a final state where glass and sand are fully segregated into two bands, as indicated by a second experiment (see Fig. 3), which starts



FIG. 5. Space-time diagram for the experiment specified in Fig. 3. The distance along the tube is given in terms of the average sand grain diameter. The diagram covers 326 h (278 000 revolutions).

with this configuration as initial condition [Fig. 3(a)]. After many rotations of the tube, we observe new white bands of glass beads nucleating within the sand [Figs. 3(b)–3(d)]. Thus, in this large-aspect-ratio system, the fully segregated state is not a stable asymptotic state.

The long-term evolution of the experiments described above is shown in the space-time diagrams of Figs. 4 and 5. In both figures, one can observe that over long periods of time some bands change their widths much, while others scarcely evolve. In particular, in Fig. 4 there are black bands that maintain almost constant width and move as a whole. This drift can persist for a considerable time span, as is the case for the two leftmost bands. The diagram also shows a drifting black band that changes its drift direction (the fourth band from the right at the end of the experiment). In Fig. 4 the dynamical changes lead to the disappearance of some bands while others grow in width. In Fig. 5 the opposite process, the nucleation of bands, occurs. We point out that

band nucleation is not limited to experiments with this initial configuration. It also occurs, though rarely, at the late stages in experiments such as the one shown in Fig. 4.

There are two striking features in Fig. 5. First is the order of appearance of the nucleated bands. Second, glass bands nucleate within the sand band, whereas nucleation of sand bands in a smoothly running glassy plug is not observed. A similar asymmetry between the two types of bands is also observed in experiments starting from a homogeneous mixture, like the one shown in Fig. 4: While two neighboring white bands can exchange mass through the black band lying between them also when the latter is wide, black material is transported only through narrow white bands. These features suggest the existence of a mechanism in addition to diffusion for transfer of grains that is effective only in black bands. Considering sources that may give rise to such a mechanism, we were led to look in more detail at the different ways the two types of band flow.

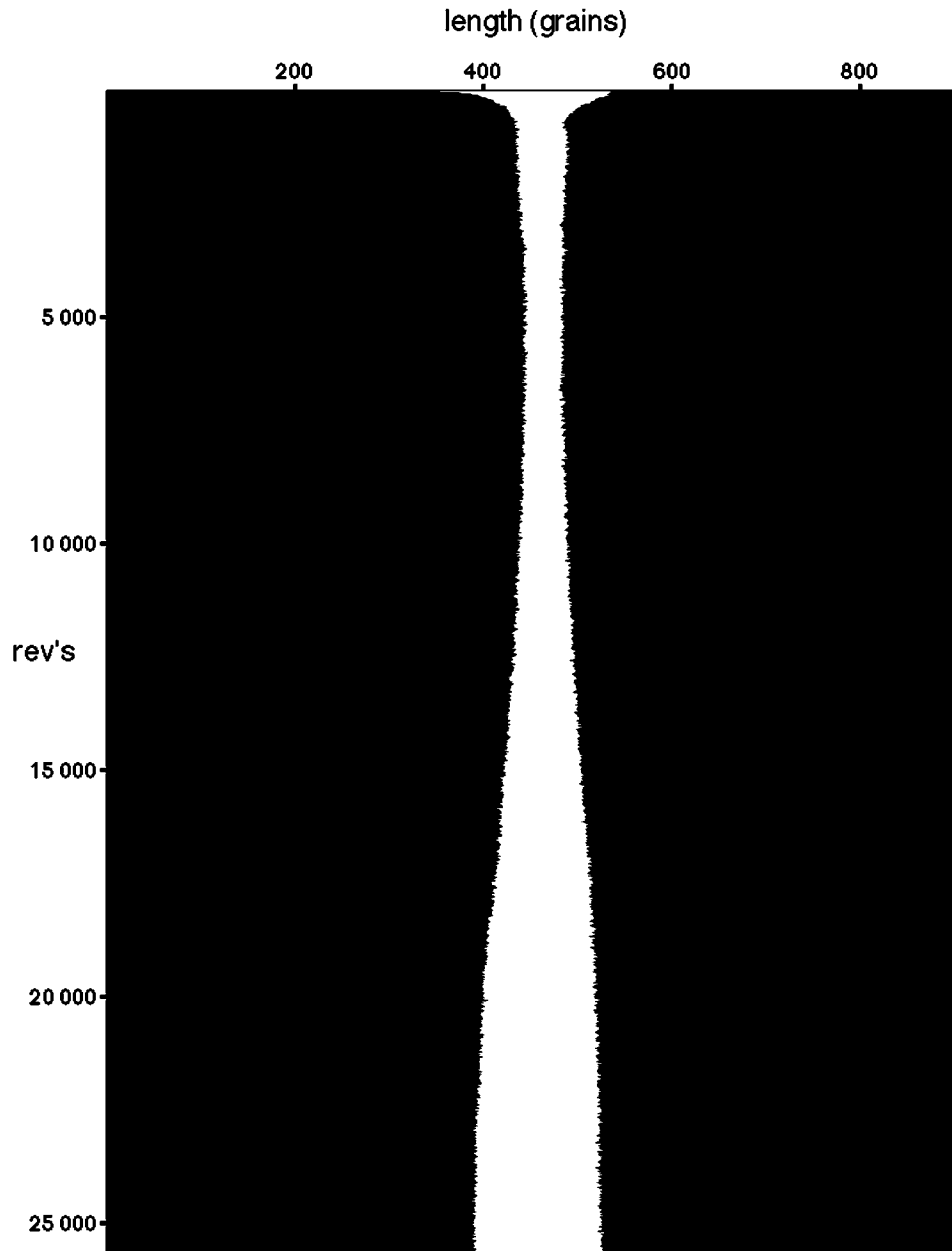


FIG. 6. An experiment with $L=16.2$ cm, 0.29-mm glass spheres, and rotation frequency 13.2 rpm. The initial configuration was a 3.4-cm-wide band of pure white material in between two bands of pure black material. The distance along the tube is given in terms of the average sand grain diameter. The space-time diagram shown covers 32.5 h (25 700 revolutions). The smallest width of the white band was 0.8 cm and the value at the end of the experiment was 2.6 cm. The velocities of the interfaces imply a flux of 1.6 sphere/rev (this estimate was obtained between revolutions 9790 and 19 300).

In wide enough sand-rich bands, avalanches do not start simultaneously all along each band. Rather, an avalanche in one location triggers a disturbance that propagates axially, which we will henceforth refer to as an *avalanche wave*. An example can be seen in the middle black band of Fig. 1, where an avalanche wave is traveling to the right. In this figure, the wave front (indicated by an arrow) has reached the middle of the band, as seen most easily from the (dark) contact area between the sand and the tube near the bottom of the tube. These avalanche waves can be surprisingly persistent, the wave pattern recurring over long periods of time.

Experiments of the type shown in Figs. 4 and 5 do not allow us to elucidate the role of avalanche waves in the band pattern dynamics for two reasons. First, in systems with

many bands, there appear to be several processes at work, as indicated by the fact that in some regions there is evolution while in others barely any. Second, our experimental resources do not allow us to resolve simultaneously the wave behavior and the evolution for large system sizes. Therefore, we performed a series of experiments with simple initial band configurations in shorter tubes to investigate whether there is a correlation between avalanche waves and transport of white material through sand-rich bands. Two crucial experiments from this series are shown in Figs. 6 and 7.

The experiment in Fig. 6 was started with a narrow pure white band between two wider bands of pure black sand. In the initial stage, which lasts for about 600 revolutions, the white band shrinks. Puzzlingly, some time later (in this case

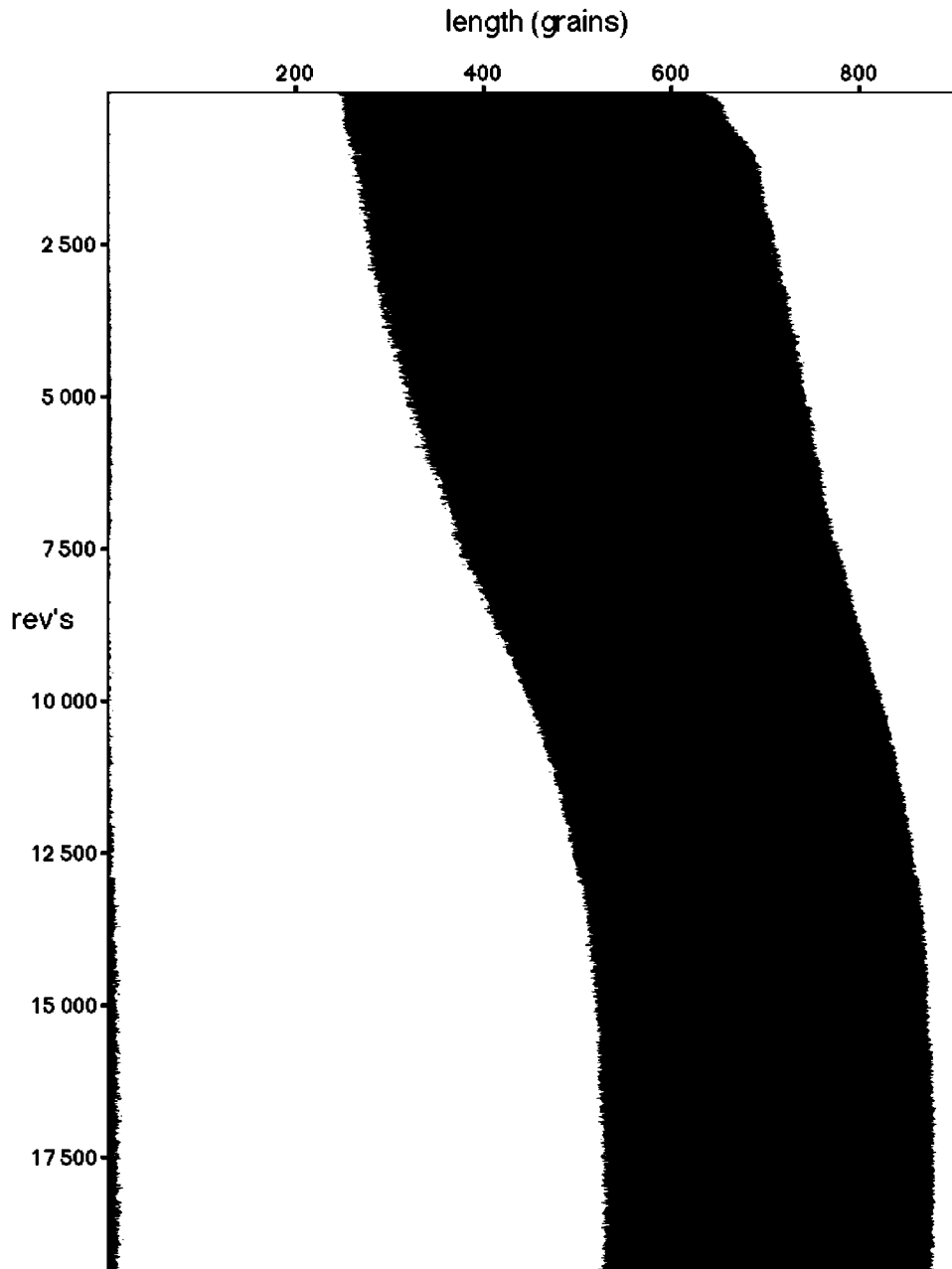


FIG. 7. Experiment with $L = 16.2$ cm, 0.29-mm glass spheres, and rotation frequency 13.2 rpm, starting from a 6.4-cm-wide black band in between two white bands. The glass bands were pure, but the black band was prepared with a gradient in concentration of white material (20% at the left edge falling off to 0% at the right edge). The distance along the tube is given in terms of the average sand grain diameter. The space-time diagram covers 24.5 h (19 400 revolutions). The experiment was continued for another 12 h (not included in the diagram), but there were no further changes in the position of the black band.

after about 7300 revolutions) the band starts to grow. It grows steadily until it has reached a width not very different from the initial one. This surprising behavior of shrinkage followed by growth is completely reproducible.

Avalanche waves may explain this peculiar, ‘bottleneck’-shaped space-time diagram. The recordings of the avalanche waves throughout this experiment reveal that initially the waves are directed towards the white band due to wave sources in the black bands, not far away from the walls. However, relatively early (after about 700 revolutions) the wave direction flips and waves now travel predominantly from the white band outward (the propagation velocity is not constant). Thus the waves seem to drain the black bands of

most of the white material that was mixed into them during the early stages of the experiment. These observations indicate that the evolution of the white band is correlated with the behavior of avalanche waves in the black bands and that the direction of transport is opposite to that of wave propagation.

The experiment shown in Fig. 7 supports further our picture of glass beads transported through a black band, opposite to the avalanche wave direction. The initial configuration here, one black band (set up with a white concentration falling off to the right) between two pure white ones, is the inverse of the one in Fig. 6. The band is steadily drifting to the right, though it never reaches the wall. This implies a

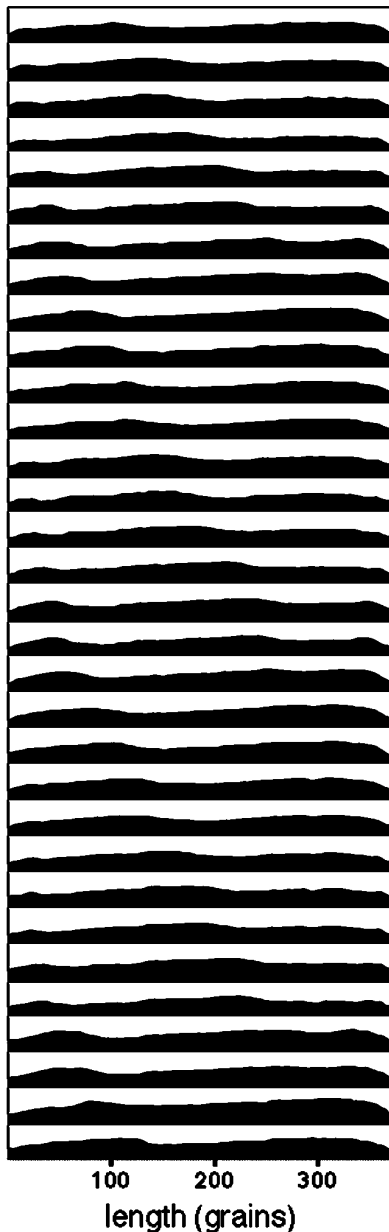


FIG. 8. Characteristic wave pattern snapshots in the black band for the experiment shown in Fig. 7. Each line shows the (dark) contact area between the sand and the tube wall near the tube bottom (see Fig. 1), as obtained from the tilted mirror underneath. Just after a local slide this area is wide (vertically). Under rotation the level diminishes (and the slope of the granular material increases), until a new slide occurs. The downward direction in the figure corresponds to increasing time. The wave triggered at the left edge of the band propagates to the right at a nearly constant velocity until it meets the left-moving wave close to the right edge of the band. The distance along the tube is given in terms of the average sand grain diameter. The sequence shown covers 1.00 s and occurred after 9540 revolutions. The period for wave emission is ≈ 0.32 s and the wave velocity 10.4 cm/s.

steady flux of glass beads through it to the left. The predominant wave direction in this experiment is to the right, as shown in Fig. 8, opposite to the transport direction. Note that the wave direction is imposed by the initial concentration gradient of glass beads in the black band (higher concentra-

tion of glass implies more frequent slides). The more pronounced fuzziness of the receding boundary compared to the advancing one, as seen in the diagram, reflects a shorter and steeper transition zone between sand and glass bands in the latter. Note the accumulation of a smaller amount of black material at the left wall. Interestingly, in the final stages of both these experiments the concentration of white in the black is the same, around 5%; see Figs. 6 and 7.

IV. DISCUSSION

A. Avalanche waves as a transport mechanism

The results presented above suggest that avalanche waves constitute an important transport mechanism driving the evolution of this system. While we cannot provide at the present time a detailed quantitative model of how glass spheres pick up systematic axial shifts opposite to the wave direction, we propose a qualitative picture of how avalanche waves may induce transport.

Consider the surface shape of an avalanche front propagating to the right as shown in the middle black band of Fig. 1. To the left, behind the front (which is indicated by an arrow), the tube rotation has already increased the local slope and thus the contact area is more narrow (vertically). As one moves towards the front, the slope gradually decreases since the passage of the avalanche has taken place more recently. Finally, just on reaching the top of the front, the slope is the smallest since the avalanche has just relaxed it from the threshold of instability. In contrast, the region just to the right of the front is characterized by the steepest slope, which the avalanche is about to relax, and here the contact area is at its narrowest. This change of slope from the smallest to the highest value takes place over a small length scale, typically 30 in terms of the sand grain diameter. A glass bead reaching the surface will therefore, for most of its transit time down, find itself in regions behind avalanche waves, where the steepest-descent vector on the sand surface has an axial component to the left. Following the frozen slope [17,18], the glass bead will therefore shift slightly in the axial direction opposite to wave propagation. If, on the other hand, the glass bead happens to be caught by an avalanche, it will be carried by it down without any systematic shift in the axial direction. The net result is an axial flux of glass beads opposite to the direction of wave propagation.

Another important element in our picture is the inherently noisy nature of avalanches in our system. After an avalanche, the irregular sand grains at the bottom of the slope build kinetically arrested configurations, which do not necessarily correspond to energy minima. Therefore, the triggering of avalanche waves at a particular location is not entirely periodic, as we indeed observe, but fluctuates. This is particularly striking in tubes containing only sand, where wave patterns change in a matter of a few seconds. By contrast, in sand bands flanked by glass bands, where waves are triggered predominantly at the boundaries, wave patterns are much more persistent. We conjecture that the continuous flow in the adjacent glass bands, together with the larger concentration of glass beads in the sand band near the boundaries, may facilitate the instability leading to wave triggering in those regions.

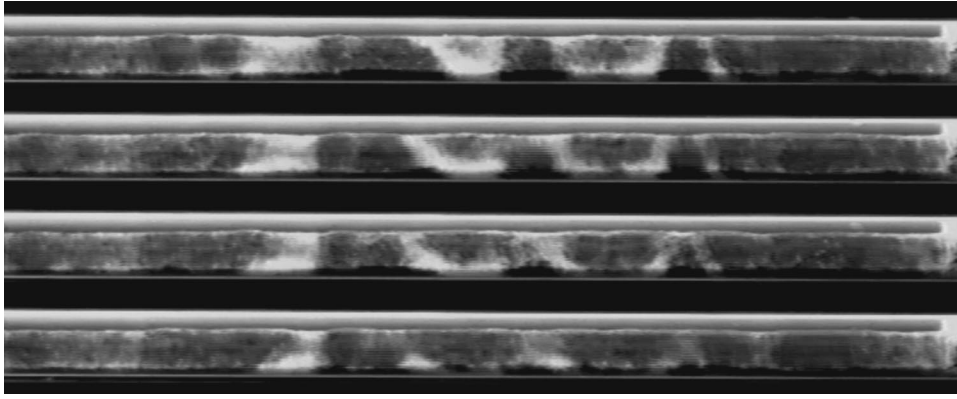


FIG. 9. Early stages of band formation from a mixture of black sand and 0.29-mm glass spheres. The system size was $L = 16.2$ cm and the angular velocity 13.1 rpm. The series of images shown occurred after 9 revolutions and they span 0.14 revolutions. Note also the irregular behavior of avalanches in the sand-rich regions, as seen along the lower contact line (dark area). This behavior arises due to the lack of triggering by developed white bands.

We can put now all the elements of our picture together. Consider an entire sand band, such as the one corresponding to Fig. 7. Due to the stochastic nature of avalanche triggering, the waves that originate at the two edges of the band lack phase coherence. As a consequence of this and variations in the velocity of propagation, these counterpropagating waves meet at a point whose location along the band fluctuates stochastically. While in some cases it may fluctuate near the middle of a band, in others it is clearly displaced towards one side (as is the case for the experiment in Fig. 7). One may conjecture that the effects of the waves traveling in opposite directions would cancel out, also when the meeting point is systematically displaced from the center. However, we observe that there is transport opposite to the dominant wave direction, consistent with the mechanism outlined above. We point out that a drift of the meeting point from one side of the band to the other may also account for the reversal in transport seen in some of our experiments (see Fig. 4). Our picture may also explain another feature that we often observe: Glass beads seem to be transported more efficiently across wide sand bands than narrow ones. In a narrow band, the slope is relaxed simultaneously all across and thus no wave propagation occurs.

B. Nucleation and disappearance of bands

The different mobilities of the sand grains and the glass spheres are crucial for the transport mechanism outlined above. In order to elaborate somewhat on this point, we present here some observations on the early stages of band nucleation. After just a few rotations, a nearly homogeneous mixture develops concentration inhomogeneities. Figure 9 shows this stage in detail. This is a rather fast process, a result of the fact that the mixture was initially heavily supersaturated with the white material. In their early stages these incipient bands do not fill the cross section (see Fig. 9). They rotate with the mixture and concentrate in space each time they slide down the surface (these collections of glass beads tend to slide faster than the mixture). Since they do not fill the cross section, the incipient bands show up as horizontal white stripes in a space-time diagram (Fig. 10), approximately twice for each rotation of the half-filled tube. When enough white material has accumulated a continuous white

band is formed. We cannot rule out that these glass bands have a core of the less mobile sand grains as suggested in Ref. [10]. The collective motion of spheres in incipient bands is influenced by the tube rotation frequency. We found that narrower bands (and a larger number of them) are formed in experiments at higher frequency. The opposite tendency has been reported for sand-sand mixtures [5,8,12]. In our system nucleation of bands occurs independently of whether there are avalanches (lower frequencies) or a continuous flow (higher frequencies) in the mixture. We have not yet investigated whether there is coarsening of the band pattern in this high-frequency regime.

Finally, some words about band disappearance are in order. When a white band has lost sufficient mass, the “reverse” process of the nucleation occurs. An azimuthally inhomogeneous collection of white material is formed from the continuous band, and during rotation white grains are pumped into the surrounding black bands. We often observe the disappearing band to move towards a neighboring white band (see also Fig. 4). We note that the shrinkage and disappearance of a band is a much slower process than band formation. The high concentration of white material in the surrounding black bands after a white band has disappeared decays relatively fast, as indicated by a fast widening of the (white) neighbor.

V. SUMMARY

We have presented a study of the long-term evolution of one-dimensional patterns produced by the segregation of binary mixtures of glass beads and sand grains in half-filled rotating horizontal tubes. After bands are created, they undergo a coarsening process by which some bands shrink and disappear while others grow at their expense. Our observations indicate that this coarsening process saturates and a steady state is reached. While previous authors have tried to account for segregation and the ensuing evolution in terms of a diffusion process with a negative diffusion coefficient, our findings suggest that other transport mechanisms may be at work. In trying to identify one of these, we were led to consider the differences in flow between the two constituent powders: While glass beads fall smoothly along the rotation-

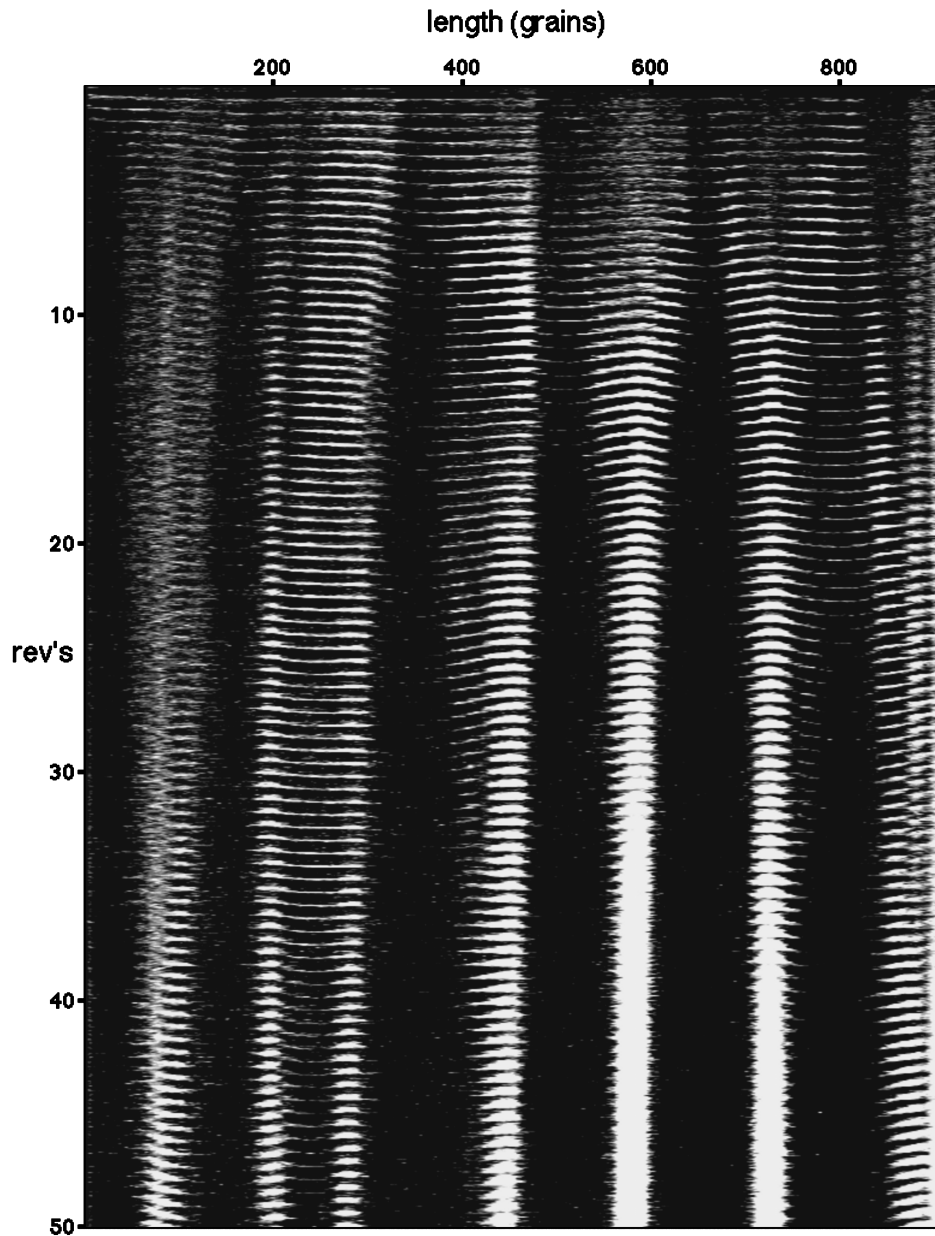


FIG. 10. Early stages of band formation for the same experiment as in Fig. 9. The distance along the tube is given in terms of the average sand grain diameter. This space-time diagram covers the first 50 revolutions of the experiment. Inhomogeneous collections of white material grow until continuous bands are formed. Note the different temporal behavior of the incipient bands.

generated slope, sand flow is punctuated by avalanches that propagate axially. Our experiments using simple band configurations show that glass beads are transported across wide sand bands, while transport of sand grains across glass bands seems minimal. Therefore, we conclude that propagating avalanches may be responsible for transport. We have provided evidence that glass beads are transported across a sand band in a direction opposite to the dominant avalanche wave. We believe that this transport mechanism is important in determining the evolution also in the general case. Propagating avalanche disturbances are asymmetric and have a noisy character. This hints at similarities with transport models based on thermal ratchets studied recently [19].

In this exploratory study, we have kept relevant parameters such as the type (smooth or rough) and relative sizes of the grains, the tube diameter and length relative to the grain

size, the filling fraction, and the rotation frequency fixed. Future studies should address the effects of their variation on nucleation and evolution. We cannot rule out the influence of other, uncontrolled, parameters such as variations in the tube diameter since small perturbations such as these will be amplified under many rotations [11].

ACKNOWLEDGMENTS

We are grateful to Stefan Thomae for an engaging series of discussions throughout this project. This study was supported by Grant No. 92-00093/2 from the U.S.–Israel Binational Science Foundation, Jerusalem, Israel. V.F. gratefully acknowledges support from The Research Council of Norway (NFR).

- [1] S. B. Savage and C. K. K. Lun, *J. Fluid Mech.* **189**, 311 (1988).
- [2] R. Jullien and P. Meakin, *Nature (London)* **344**, 425 (1990).
- [3] A. D. Fitt and P. Wilmott, *Phys. Rev. A* **45**, 2383 (1992).
- [4] L. Prigozhin, *Chem. Eng. Sci.* **48**, 3647 (1993).
- [5] Y. Oyama, *Bull. Inst. Phys. Chem. Res. Jpn. Rep.* **18**, 600 (1939). Oyama's work was reported by S. S. Weidenbaum, in *Advances in Chemical Engineering*, edited by T. B. Drew and J. W. Hoopes (Academic, New York, 1958), Vol. 2, p. 211.
- [6] M. B. Donald and B. Roseman, *Br. Chem. Eng.* **7**, 749 (1962); **7**, 922 (1962).
- [7] J. Bridgewater, N. W. Sharpe, and D. C. Stocker, *Trans. Inst. Chem. Eng.* **47**, 114 (1969).
- [8] S. Das Gupta, D. V. Khakhar, and S. K. Bhatia, *Chem. Eng. Sci.* **46**, 1513 (1991); *Powder Technol.* **67**, 145 (1991); S. J. Rao, S. K. Bhatia, and D. V. Khakhar, *ibid.* **67**, 153 (1991).
- [9] K. M. Hill and J. Kakalios, *Phys. Rev. E* **49**, R3610 (1994); **52**, 4393 (1995).
- [10] K. M. Hill, A. Caprihan, and J. Kakalios, *Phys. Rev. Lett.* **78**, 50 (1997).
- [11] O. Zik, D. Levine, S. G. Lipson, S. Shtrikman, and J. Stavans, *Phys. Rev. Lett.* **73**, 644 (1994).
- [12] M. Nakagawa, *Chem. Eng. Sci.* **49**, 2540 (1994).
- [13] S. B. Savage, in *Disorder and Granular Media*, edited by D. Bideau and A. Hansen (Elsevier, Amsterdam, 1993), p. 255.
- [14] G. Baumann, I. M. Jánosi, and D. E. Wolf, *Europhys. Lett.* **27**, 203 (1994); *Phys. Rev. E* **51**, 1879 (1995).
- [15] T. Boutreux and P. G. de Gennes, *J. Phys. I* **6**, 1295 (1996).
- [16] G. Metcalfe, T. Shinbrot, J. J. McCarthy, and J. M. Ottino, *Nature (London)* **374**, 39 (1995).
- [17] G. H. Ristow, F.-X. Riguïdel, and D. Bideau, *J. Phys. I* **4**, 1161 (1994).
- [18] F.-X. Riguïdel, A. Hansen, and D. Bideau, *Europhys. Lett.* **28**, 13 (1994); F.-X. Riguïdel, R. Jullien, G. H. Ristow, A. Hansen, and D. Bideau, *J. Phys. I* **4**, 261 (1994).
- [19] L. P. Faucheux, L. S. Bourdieu, P. D. Kaplan, and A. J. Libchaber, *Phys. Rev. Lett.* **74**, 1504 (1995).